

Analysis of Local Flame Propagation in Gas Explosions with Multiple Obstacles

D.J. Park¹, A.R. Green¹ and Y.C. Chen²

¹School of Safety Science, Faculty of Science, The University of New South Wales, NSW 2052, AUSTRALIA

²School of Mechanical & Manufacturing Engineering, Faculty of Engineering, The University of New South Wales, NSW 2052, AUSTRALIA

Abstract

Experimental investigations were performed in a top-venting explosion chamber to assess the effects of multiple obstacles on local flame propagation. The chamber dimension is 235 mm in height with a 1000 × 950 mm² rectangular cross section and a large vent area of 1000 × 320 mm². Multiple cylindrical obstacles with blockage ratio of 30 % were used. Temporally resolved flame front images were recorded by a high speed video camera to investigate the interaction between the propagating flame and the obstacles. The propagation velocity of local flame fronts around the obstacles was estimated.

Introduction

Gas explosions have a considerable implication on the safety in terms of potential loss of life, asset and business interruption risks. In particular, explosions occurring in confined and partially-confined regions of are of special concern due to the potential for domino effects and more serious consequences [1]. The interaction between the flame and the local blockage caused by the presence of equipments such as pip-work and vessels causes local flame acceleration of the propagating flame front [2]. The influences of such local blockage on explosion process were performed through laboratory-scale studies by many investigators [3,4,5,6].

The studies based on large length to diameter (L/D) ratio revealed that there is a strong interaction between the turbulence level formed behind the obstacle and the resulting peak pressure, and the turbulent flame and turbulence interaction trapped behind the obstruction greatly enhance the speed of flame propagation and hence increase the rate of pressure rise. However, the more detailed data of the flame displacement velocities due to the propagating flame front and obstacles have not been reported.

The present work aims at providing the experimental data of the local flame propagation velocities around the obstacle and investigating the underlying mechanisms of local flame/obstacles interactions in a partially confined enclosure with small L/D ratios and a large vent area.

Experimental Set-Up

Figure 1 shows a schematic diagram of the experimental set-up consisting of an explosion chamber, 235 mm in height, 1000 × 950 mm² in cross section and with a large top-venting area of 1000 × 320 mm². This gives a total volume of 223 liters of explosive mixture and a $A_v/V^{2/3}$ ratio of 0.8695. The rig was made of 20 mm thick transparent chemiglass restrained by bolted flanges and strong adhesives. Flammable gas (99.95 % CH₄ by vol.) entered the box through the valve placed in the bottom of the side wall of the chamber. The fuel volume flow rates were monitored using a calibrated gas flow control system (TEI, Model GFC 521).

Before gas filling, the large rectangular vent of area 1000 × 320 mm² was covered with thin plastic film (household plastic wrap). The film was sealed on a layer of blue tar lined around the vent. Air within the chamber during the filling sequence was continuously withdrawn via the open sample ports positioned at three different locations. The fuel/air mixture was circulated through the explosion chamber using a recirculation pump for several minutes to ensure a completely homogeneous mixture and then allowed to settle for several minutes before ignition. The fuel concentration was monitored by an infrared gas analyzer (GDA, Model LMSx) with an accuracy of ± 0.3%. The calibration of the apparatus was periodically checked by injecting calibration gases of known composition into the measurement system.

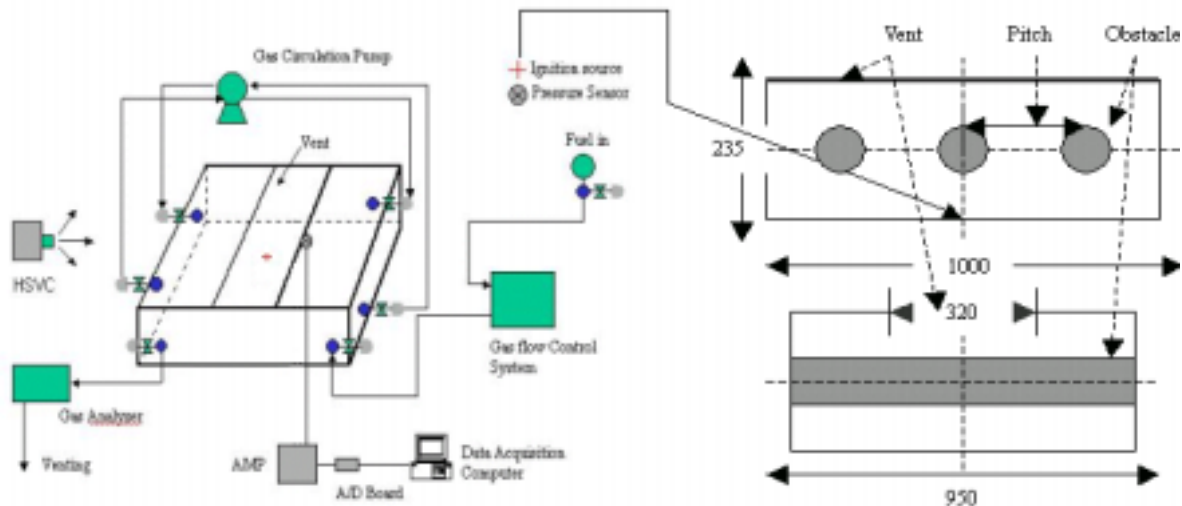


Figure 1: Schematic diagram of the experimental arrangements and the rig.

The flammable mixture in the chamber was ignited by a 15.5 KV electric spark positioned near the centre of the bottom wall, when the contact switch was closed. The flame images were photographed with a high speed video camera (KODAK Motion Recorder Analyzer, SR-ULTRA-C) operating at the rate of 500 frame/s, providing a temporal resolution of 2 ms. The pressure was recorded using a dynamic pressure transducer with a range of 0-2.5 bar (KISTLER type 701 A). Signals from the pressure transducer were logged on a 16 bit A/D converter sampling at 2 kHz, and a channel charge amplifier (KISTLER type 5019 B) and data acquisition computer were used to record pressure data.

As shown in figure 1, multiple solid obstructions with blockage ratio of 30% were mounted inside the chamber and centred 117.5 mm from the bottom of the chamber. The estimation of blockage ratio is an area percentage defined as the largest cross-sectional area blocked by positioning the obstruction in the explosion chamber divided by the cross-sectional area of the explosion chamber which is $1000 \times 950 \text{ mm}^2$ [5].

The methane concentration in air was $(10 \pm 0.2) \%$, a slightly richer mixture than a stoichiometric methane/air mixture. Each test was repeated at least five times in order to ensure reproducibility and the results were averaged and the average results were presented. The reproducibility between all tests was found to be reasonable: the error was $\pm 5\%$ in time and $\pm 5\%$ in pressure.

Image Processing and Flame Front Tracking

The procedures to study the local flame-front characteristics are divided into the following three steps:

(1) Identification of the region of interest.

As shown in Fig. 2 (a), the local region of interest selected here was around the left obstacle. The sub-region area was $100 \times 100 \text{ pixels}^2$ with the centre of the obstacle coincide with that of the region of interest.

(2) Image processing.

Fig. 2 (b) shows one example of image processing applied in the area of interest to the original flame image obtained at 120ms after ignition. Image analysis was done by using the Optical Multi-channel Analyser (OMA) program for all the images obtained from the high speed video camera. A 5 by 5 smoothing filter is applied initially before the image is made binary. The red colour represents the burnt area and the block one is the unburnt area including the circular obstacle. A sequence of images can be processed to study the flame propagation behaviour at the vicinity of the obstacles and the flame-front boundary is determined for each individual image.

(3) Flame front tracking.

The flame-front contour coordinates of each image can be extracted by using an in-house FORTRAN code. All points along the contour are separated by 1 pixel, and one pixel here is 2 mm. With the coordinates of the contour, the flame front length and local flame front displacement in the normal direction between two consecutive images were calculated. Local flame propagation velocity was determined along the flame front by dividing the distance along the normal line at each point by the time between images.

Results and Discussions

Figure 3 shows a sequence of temporally resolved flame-front images in the region of interest. The time shown below each image represents the elapsed time after ignition and subsequent flame images are at 2 ms intervals.

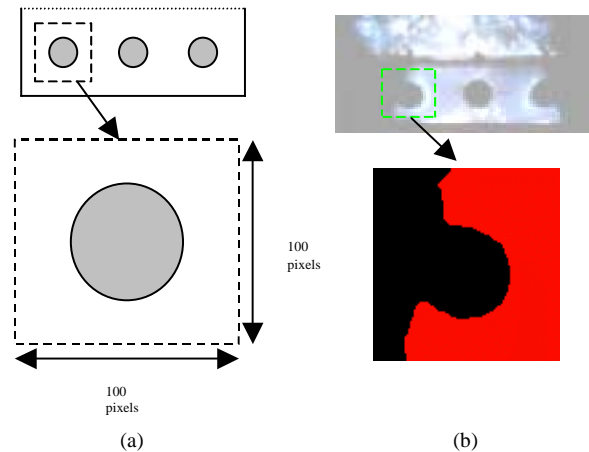


Figure 2: (a) Selection of a local area of interest; (b) Example of image processing applied to the original flame image in the area of interest.

The propagating flame front moves laterally toward the left obstacle and reaches the right side of the obstacle at about 96 ms after ignition. After impinging on the obstacle, the segment of flame front above the obstacle was found to propagate slower than the lower segment of the flame front.

With increasing time after impingement, the flame starts to roll up around the obstacle, and the flame decelerates. This is seen in figure 4 (a) where the temporal increase of the burnt area, A , slows down slightly with time. After flame deceleration, the flame burns into the wake and the propagation flame front reconnects, the flame accelerates again. The flame surface area is greatly increased at this stage and hence the burning rate. Flame reconnection in the wake of the obstacle occurred at about 134 ms after ignition.

Figure 4 (b) shows a comparison of the average of the local flame propagation velocity, S_{av} , derived via two different methods from 80 ms to 140 ms after ignition. The first one is from the incremental burnt area, ΔA , divided by the flame front length, L ; the second is from the average of the local propagation velocity determined at each point along the flame front. In the first method, the flame front length touched with the obstacle is not included at the calculation of the flame front length. The results from both methods show good consistency, as expected.

The local flame propagation velocity remains fairly constant at approximately 2 m/s before the flame impinges onto the obstacle. The much higher value of the flame propagation velocity than the laminar burning velocity is due to the expansion effect as actually it is the burnt gas velocity that is measured here.

Much higher burning velocity is found at the early stage of flame impingement onto the obstacle. Despite some fluctuations, the general trend of the local propagation velocity is decreasing when the flame passes over the obstacle from 96 ms to 126 ms after the ignition. Only when the flame has passed over the obstacle does the local burning velocity rise again most likely due to turbulent generated at the wake of the obstacle.

Conclusions

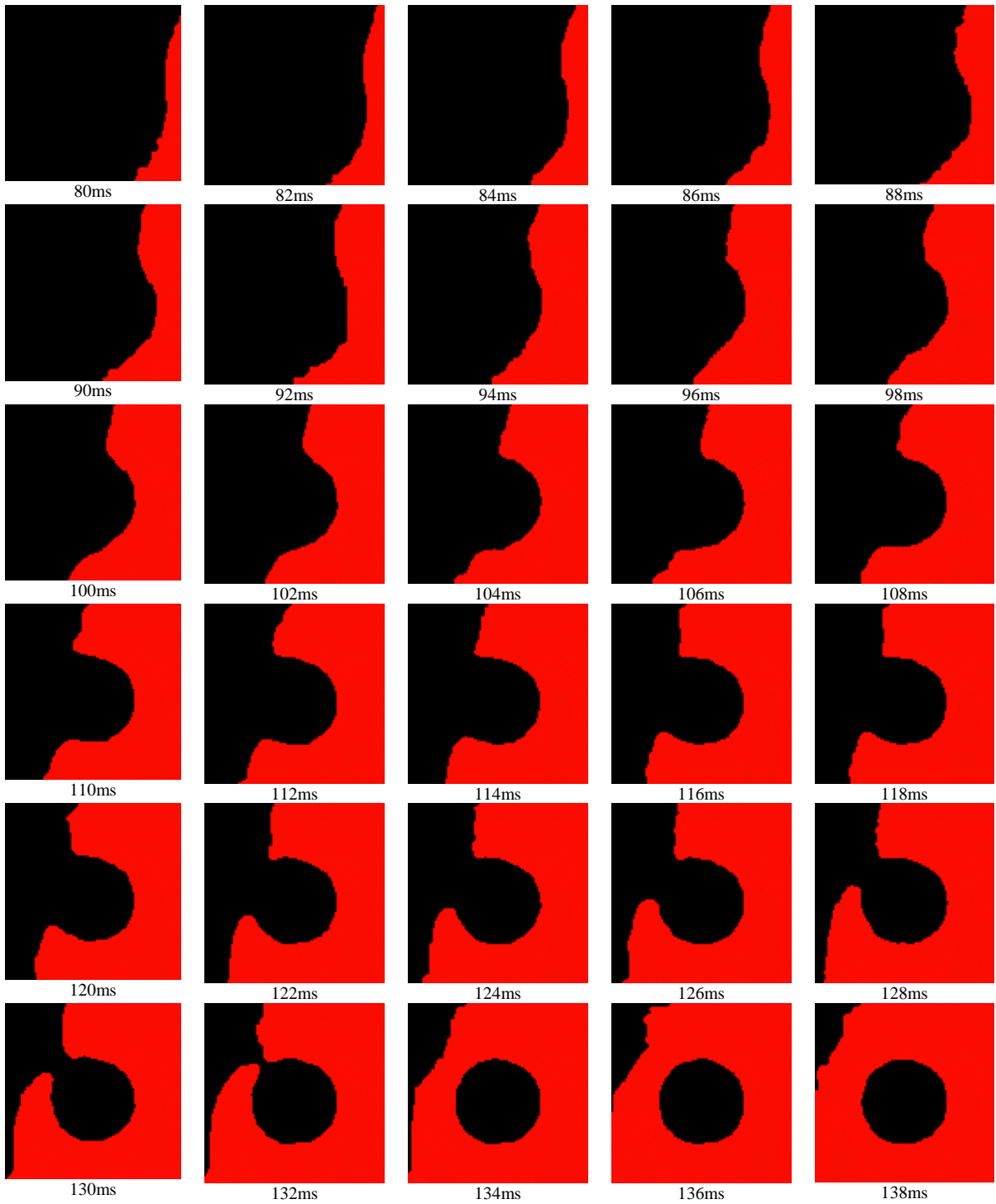
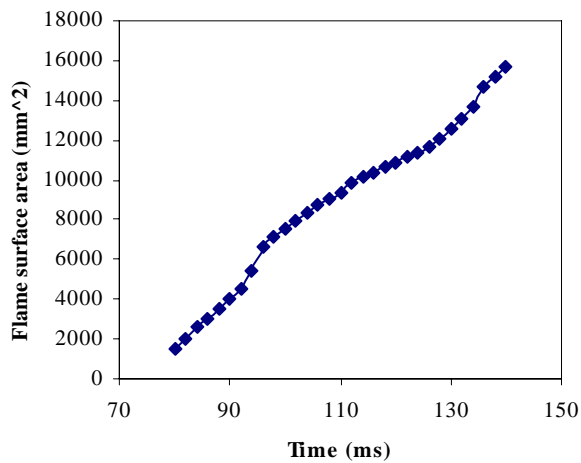
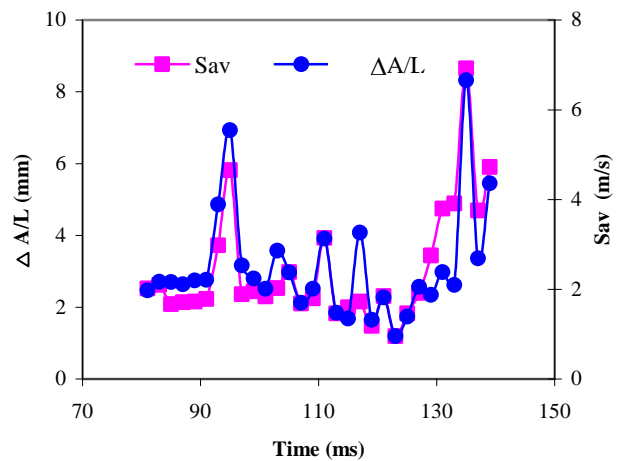


Figure 3: A temporal sequence of flame-front images in the region of interest showing flame propagation around the left obstacle during the course of the explosion.



(a)



(b)

Figure 4: (a) The flame area of local burnt area with time and (b) The incremental burnt area (ΔA) divided by the flame front length (L) and the average of the local flame propagation velocity (S_{av}) versus time after ignition for the local area

High-speed images have been acquired for a propagating premixed flame interacting with multiple obstacles in an explosion chamber. The images were processed to obtain the temporally resolved flame-front contours in the region of interest around the obstacle. An in-house FORTRAN code is further developed to determine the local flame propagation velocity.

The results show that overall the flame propagation slows down slightly after impinging onto the obstacle and accelerates again after flame front reconnection. The average of the local flame propagation velocity increases drastically when the flame impinges onto the obstacle. It follows then a decreasing trend and rises again after flame reconnection behind the obstacle wake.

Acknowledgments

The authors gratefully acknowledge the financial support by R&D Training Centre, Korea Gas Corporation.

References

- [1] Green, A.R. & Nehzat, N., Experimental studies of flame propagation and pressure rise in a 1:54 scale coal mine model, *Australian Symp. on Combustion and The Sixth Australian Flame Days*, 1999, 170-174 August..
- [2] Hargrave, G.K., Jarvis, S.J. and Williams, T.C., A study of transient flow turbulence generation during flame/wall interactions in explosions, *Meas. Sci. Technol.*, **13**, 2002, 1036-1042.
- [3] Moen, I.O., Donato, M., Knystautas, R. & Lee, J.H., Flame Acceleration Due to Turbulence Produced by Obstacles, *Combust. Flame*, **39**, 1980, 21-32.
- [4] Masri, A.R., Ibrahim, S.S., Nehzat, N., & Green, A.R., Experimental study of premixed flame propagation over various solid obstructions, *Experimental Thermal and Fluid Science*, **21**, 2000, 109-116.
- [5] Ibrahim, S.S. & Masri, A.R., The effects of obstructions on overpressure resulting from premixed flame deflagration, *J. Loss Prev. in the Process Ind.*, **14**, 2001, 213-221.

- [6] Phylaktou, H., & Andrews, G.E., Gas Explosions in Long Closed Vessels, *Combust. Sci. and Tech.*, **77**, 1991, 27-39.